Article ID: 1001-3555(2017)04-0299-06

Formation of Helium-3 and Helium-4 during Photocatalytic Hydrogen Generation over Cadmium Sulfide under Visible Light Irradiation

LU Gong-xuan[1,*], ZHEN Wen-long[1,2]

(1. *State Key Laboratory for Oxo Synthesis and Selective Oxidation, Lanzhou Institute of Chemical Physics, Chinese Academy of Science, Lanzhou* 730000, *China*;
2. *University of Chinese Academy of Science, Beijing* 100049, *China*)

Abstract: Here, we report that small amount of ^{3}He and ^{4}He can be produced during photocatalytic hydrogen generation over cadmium sulfide (CdS) semiconductor suspension under visible light irradiation. This work raises a possible route to generate ^{3}He and ^{4}He from proton in the water under very mild conditions through low-energy nuclear reaction (LENR).

Key words: photocatalytic hydrogen generation; formation of Helium-3 and Helium-4; CdS semiconductor suspension; visible light irradiation

CLC number: O643.32 **Document code**: A

Nowadays, ^{3}He has been recognized as an efficient, clean, safe, inexpensive nuclear fusion power generation fuel[1-5]. However, the amount of ^{3}He on the earth is very limited, only around 500 kg. It is believed that helium can only be generated in nuclear reaction under very high temperature and high pressure. Truran, Hansen and Cameron investigated the enrichment of helium over long periods of time by stars of conventional mass, about 20×10^9 years[6-7]. But the fusion in the stars cannot account for the abundance of helium in the universe. Nevertheless, there are several unclear phenomena which cannot be explained by our up to date knowledge. For example, scientists found that there were excess ratios of ^{3}He and ^{4}He in submarine hydrothermal water[8]. The observation of energy balance of Jupiter seems also indicate the possibility of low energy fusion reaction there[9]. Besides, previous electrolysis experiments presented measurable amounts of ^{4}He[10]. In that experiment, Miles et al. found ^{4}He could be formed via electrochemical route from D_2O using palladium cathodes[11]. Jung also reported the production of helium and long-living radioactive isotopes by protons with 8, 16 and 24 MeV and by deuterons with 9 and 14 MeV in foils of high purity Al, Ti, V, Fe, Ni, Cu and an AISI-316 type stainless steel[12].

In our previous work, we found that small amount of deuterium and helium can be produced during photocatalytic hydrogen evolution from water catalyzed by Pt-graphene under visible light irradiation in Br-dye sensitization system[13]. In this work, we found that ^{3}He and ^{4}He could be produced during photocatalytic hydrogen generation in Pt/CdS semiconductor suspension under visible light irradiation. The detected amount of H_2, ^{3}He and ^{4}He increased with irradiation time increase. These results indicate that proton can be converted to helium under very mild condition, under far below the nuclear fusion reaction condition, therefore, is very important because it may account for the difference between the estimated He abundance and

Received date: 2017-05-28; **Revised date**: 2017-06-20.

Foundation: The National Natural Science Foundation of China (Grant No. 21433007 and 21673262) and the 973 Program of Department of Sciences and Technology China (Grant No. 2013CB632404).

First author: LU Gong-xuan(1964-), PhD, Researcher. E-mail: gxlu@lzb.ac.cn, Tel: +86-931-4968178.

Corresponding author: E-mail: gxlu@lzb.ac.cn. Tel.: +86-931-4968178.

measured He abundance in our universe, no matter the generation rate is high or low.

1 Experiments section

1.1 Materials

All chemicals were commercial purchased and used without further purification. Cadmium nitrate ($Cd(NO_3)_2 \cdot 4H_2O$, Tianjin Kemiou Chemical Reagent Co., Ltd, AR, ≥99.0%), sodium sulfide ($Na_2S \cdot 9H_2O$, Chengdu Kelong Chemical Reagent Co., Ltd, AR, ≥98.0%), chloroplatinic acid ($H_2PtCl_6 \cdot 6H_2O$, Tianjin Kemiou Chemical Reagent Co., Ltd, AR, ≥99.0%), hydrazine hydrate($H_4N_2 \cdot H_2O$, Xilong Chemical Co., Ltd., AR, >80%), anhydrous sodium sulfate (Na_2SO_3, Xilong Chemical Co., Ltd, AR, ≥99%). De-ionized water with a specific resistance of 18.2 MΩ · cm was obtained by reverse osmosis followed by ion-exchange and filtration (Milli-Q™ Advantage A10™, France). All of the reagents were used in the experiments.

1.2 Catalyst preparation

CdS sample was prepared by a typical precipitation method[14]. Briefly, 3.5 mmol (1.0797 g) $Cd(NO_3)_2 \cdot 4H_2O$ was dissolved in 20 mL of deionized water and stirred vigorously for 60 min, 7.0 mmol (1.6813 g) $Na_2S \cdot 9H_2O$ was dissolved into another 10 mL of deionized water by ultrasonication to obtain the Na_2S solution. Then the Na_2S solution was slowly added into the above-mentioned $Cd(NO_3)_2$ solution in a drop-by-drop process under vigorous stirring. After stirring for 3 h, the obtained yellow precipitate was filtrated, washed with deionized water several times, and dried at 80 ℃ for 12 h. Finally, the products were collected and ground into powder by an agate mortar for further use.

The Pt/CdS samples were prepared by *in-situ* impregnation-reduction method according to the latest reports[14-15]. The Pt loading was 1% and denoted as Pt/CdS. Briefly, 0.1980 g CdS was dispersed in water (10 mL). The dispersion solution was sonicated for about 20 min until it became homogeneous. 1.125 mL H_2PtCl_6 solution (9.1 mmol/L) was added to the above-mentioned CdS dispersion solution. The mixture was stirred in half an hour, and then a calculated amount of hydrazine hydrate was dropped into the solution. After complete reduction, the obtained dispersions were filtered, washed with water several times to remove the impurities ion. Finally, the obtained wet solids were dried in vacuum at 80 ℃ for 12 h.

1.3 Photocatalytic activities measurement

Photocatalytic experiments were performed at room temperature in a sealed Pyrex flask (184 mL) with a flat window (an efficient irradiation area of 9.8 cm^2) and a silicone rubber septum for sampling. 0.1 g of catalyst and sacrificial reagents (0.1 mol/L Na_2S and 0.1 mol/L Na_2SO_3) was dispersed into 100 mL H_2O under the ultrasound treatment (25 kHz, 250 W) about 10 min. Prior to irradiation, the reactant mixture was degassed by bubbling Ar gas for 40 min. The Xenon lamp (HSX-UV 300, NBeT) with a 420 nm cut-off filter was used as a light source to trigger the photocatalytic reaction and was positioned 15 cm away from the reactor. The amount of hydrogen evolution was measured using gas chromatograph (Agilent 6820, TCD, 13 X columns, Ar carrier). A continuous magnetic stirrer was applied at the bottom of the reactor in order to keep the photocatalyst in suspension status during the whole experiment. The detection of H_2 and He were carried out in a GC-MS (Aglient, 5975C, Triple-Axis Detector), a Quadrupole Mass Spectrometer (LC-D200M), and a Rare Gas Isotope Mass Spectrometry System (Nobleless SFT).

1.4 Characterization of the catalysts

The powder X-ray diffraction patterns (XRD) of the samples were recorded on a Rigaku B/Max-RB X-ray diffractometer with a nickel-filtrated Cu Kα radiation in the 2θ ranging from 10° to 80° and a position sensitive detector using a step size of 0.017° and a step time of 15 s at 40 mA and 40 kV. X-ray photoelectron spectroscopy (XPS) analysis was performed using a VG Scientific ESCALAB 250Xi-XPS photoelectron spectrometer with an Al Kα X-ray resource. The binding energies were calibrated by the C 1*s* binding energy of 284.7 eV. Transmission electron microscopy (TEM) and HRTEM images were taken with a Tecnai-G2-F30 field emission transmission electron microscope

operating at accelerating voltage of 300 kV.

2 Results and discussion

The crystal structures of samples were studied using XRD , the data showed in Fig. 1. The CdS and Pt/CdS catalysts showed similar typical peaks from 10° to 80°. It is clear that the diffraction peaks of the CdS and Pt/CdS samples could be indexed to the cubic CdS phase (JCPDS # 10-0454). The peaks at 26. 5°, 43. 9°, 52. 1° and 70. 5° are attributed to the diffraction of the (111), (220), (311) and (331) crystal planes of cubic CdS, respectively[16]. No diffraction peaks characteristic of Pt was observed because of their small particle size and low loading amounts[17-18].

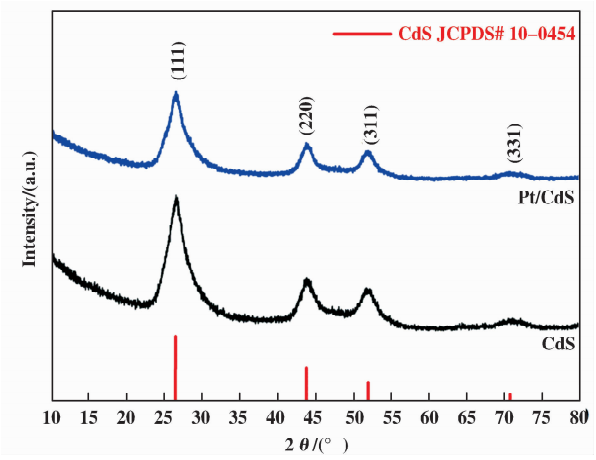

Fig. 1 XRD patterns of the CdS and Pt/CdS catalysts in the 2θ range from 10° to 80°

The surface Cd, S and Pt species on CdS and Pt/CdS catalysts were examined by XPS measurements and results were given in Fig. 2. Fig. 2a showed XPS survey (wide-scan) spectra confirmed the existence of Cd, S and C elements over CdS and Pt/CdS. The binding energies at 405. 1 and 411. 9 eV were assigned to the characteristic peaks of Cd $3d_{3/2}$ and Cd $3d_{5/2}$, respectively, indicative of Cd^{2+} in catalysts (as shown in Fig. 2b). More importantly, a spin-orbit separation

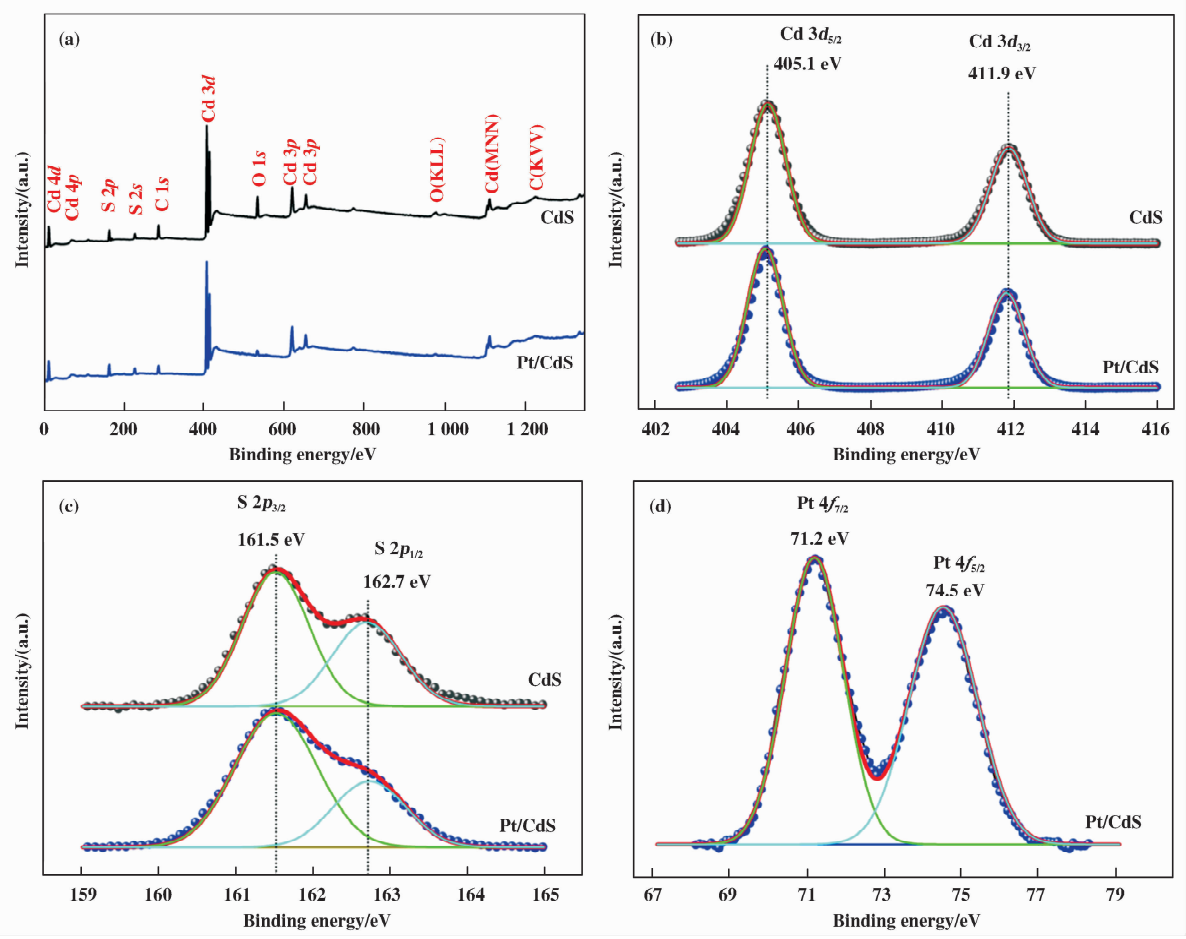

Fig. 2 (a) XPS survey, (b) Cd 3*d* and (c) S 2*p* XPS spectra of CdS and Pt/CdS samples; (d) Pt 4*f* XPS spectra of Pt/CdS sample

of 6.8 eV between Cd $3d_{3/2}$ and Cd $3d_{5/2}$ could further confirm the existence of Cd^{2+} on the surface of CdS nanoparticles[19]. Fig. 2c denoted the XPS spectrum of S $2p$, the peaks located at 162.7 and 161.5 eV could be ascribed to the characteristic peaks of S $2p_{1/2}$ and S $2p_{3/2}$ spin-orbit components of S^{2-}, respectively, further implied that S^{2-} was the main existing form on the surface of CdS and Pt/CdS samples for S element[14]. In Fig. 2d, the binding energies of 71.2 and 74.5 eV were associated with Pt $4f_{7/2}$ and Pt $4f_{5/2}$, respectively, demonstrating that the Pt precursors could be reduced to metallic Pt over Pt/CdS sample.

Moreover, the structure and morphology of Pt/CdS catalyst was studied by TEM technique (see Fig. 3a). Analysis of the CdS and Pt particles over Pt/CdS sample by HRTEM images implied that the d-spacing

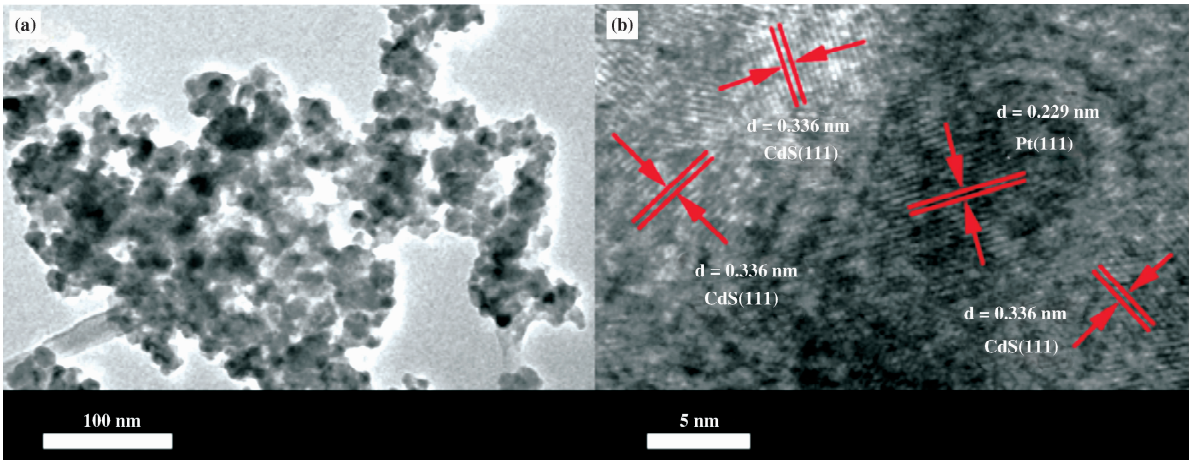

Fig. 3 TEM (a) and HRTEM (b) images of Pt/CdS catalyst

of two adjacent faces was 0.336 and 0.229 nm (Fig. 3b). This value were in agreement with the spacing of CdS (111) and Pt (111) planes, respectively[14,20]. These results are in good agreement with the results of XPS and XRD.

Fig. 4 shows the time curves of products during photocatalytic hydrogen generation. With reaction time increased, the formed hydrogen gradually increased.

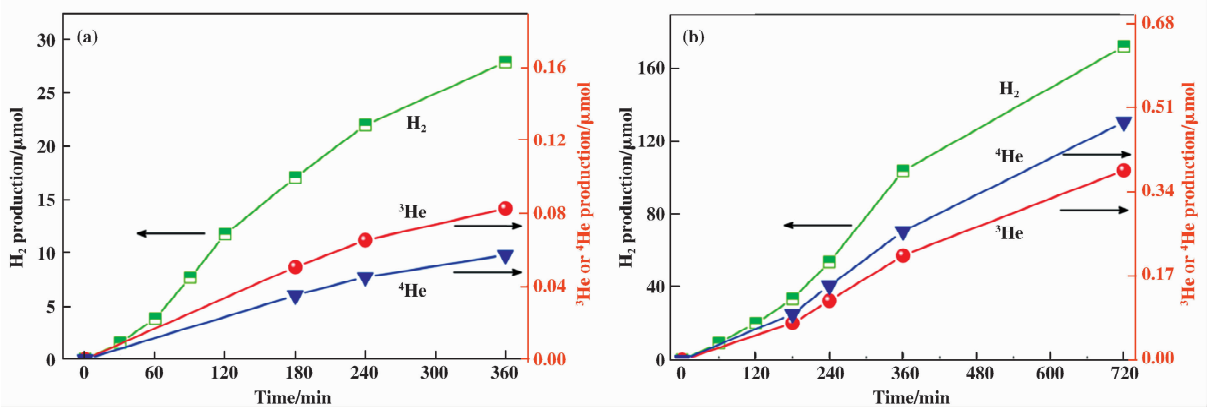

Fig. 4 The products of photocatalytic reaction over CdS (a) and Pt/CdS (b) semiconductor suspension system

Surprisingly, ^{3}He and ^{4}He were also found. The formed ^{3}He and ^{4}He were examined by a gas chromatography-mass spectrometer (GC-MS), a GC-MS (Aglient, 5975C, Triple-Axis Detector), a Quadrupole Mass Spectrometer (LC-D200M), and a Rare Gas Isotope Mass Spectrometry System (Nobleless SFT) respectively.

Obviously, it could be noted that the Pt/CdS photocatalyst had higher photocatalytic activity than CdS. 27.9 μmol of H_2, 0.083 μmol of ^{3}He and 0.057 μmol

of ^4He were produced after 360 min of irradiation over CdS samples (see Fig. 4a). In Fig. 4b, the Pt/CdS only gave 103.9 μmol of H_2, 0.211 μmol of ^3He and 0.261 μmol of ^4He after 360 min of irradiation. In addition, with the increase of the illumination time, the amount of hydrogen and helium over Pt/CdS has significantly increased. Specifically, 172.4 μmol of H_2, 0.384 μmol of ^3He and 0.482 μmol of ^4He were evolved over the Pt/CdS in 720 min. Compared with CdS itself, the Pt/CdS photocatalyst exhibits excellent photocatalytic activity for helium evolution. The hydrogen was formed by reduction of proton with light excited electron from Pt sties over CdS. During the reduction of proton by excited electron, the complex of proton and electron is electronic neutral, and this complex can further combine with electron reduced proton, i.e., hydrogen atom with some kind of electronegativity (H^-) to form deuterium and helium by low-energy nuclear reaction (LENR).

We realized that the results reported here raised more questions requiring further study. For example, the mechanism of the generation of He and of D_2 from photocatalytic water splitting is still waiting for investigation. In addition, some extra questions required further verification: (1) the exact measurement of reaction heat during He formation, (2) the detection of neutron during He formation, and (3) the specific ratio of helium isotopes should be confirmed. The detail experiments and analysis will be carried out in future.

Besides, we can make some predictions if the formation of D_2 and He follows the mechanism of the combination of proton and the H atom with some kind of electronegativity (denoted as H^-)[13], one can achieve the photocatalytic transmutation of some light nucleus to a little bit heavy nucleus, for example, synthesize Ca from K, or Ba and Pr from Cs under very mild conditions. These reactions can help us further understand the Ca formation and loss mechanism in our body and remove dangerous nuclear waste like ^{137}Cs.

Acknowledgment: This work has been supported by the National Natural Science Foundation of China (Grant No. 21433007 and 21673262) and the 973 Program of Department of Sciences and Technology China (Grant No. 2013CB632404).

References:

[1] Ongena J, Van Oost G. Energy for future centuries: prospects for fusion power as a future energy source[J]. *Fusion Sci Technol*, 2010, **57**(2T): 3-15.

[2] Yoshida N, Oh S P, Kitayama T, et al. Early cosmological H ii/He iii regions and their impact on second-generation star formation[J]. *Astrophys J*, 2007, **663**(2): 687-707.

[3] Schaeffer O A, Zähringer J. Solar flare helium in satellite materials[J]. *Phys Rev Lett*, 1962, **8**(10): 389-390.

[4] Anglin J D. The relative abundances and energy spectra of solar-flare-accelerated deuterium, tritium, and helium-3[J]. *Astrophys J*, 1975, **198**: 733-753.

[5] Möbius E, Hovestadt D, Klecker B, *et al*. Energy dependence and temporal evolution of the He-3/He-4 ratios in heavy-ion-rich energetic particle events[J]. *Astrophy J*, 1980, **238**: 768-779.

[6] Truran J W, Hansen C J, Cameron A G W. The helium content of the galaxy[J]. *Can J Phys*, 1965, **43**(9): 1616-1635.

[7] Talbot R J, Arnett W D. Helium production by pulsationally unstable massive stars[J]. *Nature*, 1971, **229**(5): 150-151.

[8] Craig H, Clarke W B, Beg M A. Excess ^3He in deep water on the East Pacific Rise[J]. *Earth Planet Sci Lett*, 1975, **26**(2): 125-132.

[9] Hanel R A, Conrath B J, Herath L W, *et al*. Albedo, internal heat, and energy balance of Jupiter: Preliminary results of the Voyager infrared investigation[J]. *J Geophys Res: Space Phys*, 1981, **86**(A10): 8705-8712.

[10] Miles M H, Bush B F, Lagowski J J. Anomalous effects involving excess power, radiation, and helium production during D_2O electrolysis using palladium cathodes[J]. *Fusion Sci Technol*, 1994, **25**(4): 478-486.

[11] Miles M H, Hollins R A, Bush B F, *et al*. Correlation of excess power and helium production during D_2O and H_2O electrolysis using palladium cathodes[J]. *J Electro Chem*, 1993, **346**(1/2): 99-117.

[12] Jung P. Helium production and long-term activation by protons and deuterons in metals for fusion reactor application[J]. *J Nucl Mater*, 1987, **144**(1): 43-50.

[13] Lu G, Tian B. Formation of deuterium and helium during photocatalytic hydrogen generation from water catalyzed by Pt-graphene sensitized with Br-dye under visible light irradiation[J]. *J Mol Catal (China)*, 2017, **31**(2):

101-104.

[14] Ning X, Li J, Yang B, *et al.* Inhibition of photocorrosion of CdS via assembling with thin film TiO_2 and removing formed oxygen by artificial gill for visible light overall water splitting[J]. *Appl Catal B*, 2017, **212**: 129-139.

[15] Zhen W, Li B, Lu G, *et al.* Enhancing catalytic activity and stability for CO_2 methanation on Ni@ MOF-5 *via* control of active species dispersion[J]. *Chem Commun*, 2015, **51**(9): 1728-1731.

[16] Ning X, Meng S, Fu X, *et al.* Efficient utilization of photogenerated electrons and holes for photocatalytic selective organic syntheses in one reaction system using a narrow band gap CdS photocatalyst[J]. *Green Chem*, 2016, **18**(12): 3628-3639.

[17] Li H, Bian Z, Zhu J, *et al.* Mesoporous Au/TiO_2 nanocomposites with enhanced photocatalytic activity[J]. *J Am Chem Soc*, 2007, **129**(15): 4538-4539.

[18] Bian Z, Tachikawa T, Kim W, *et al.* Superior electron transport and photocatalytic abilities of metal-nanoparticle-loaded TiO_2 superstructures[J]. *J Phys Chem C*, 2012, **116**(48): 25444-25453.

[19] Wang D H, Wang L, Xu A W. Room-temperature synthesis of $Zn_{0.80}Cd_{0.20}S$ solid solution with a high visible-light photocatalytic activity for hydrogen evolution[J]. *Nanoscale*, 2012, **4**(6): 2046-2053.

[20] Zhai C, Zhu M, Pang F, *et al.* High efficiency photoelectrocatalytic methanol oxidation on CdS quantum dots sensitized Pt electrode[J]. *ACS Appl Mater. Interf*, 2016, **8**(9): 5972-5980.

半导体 CdS 悬浮体系中可见光催化产氢同时生成氦-3 和氦-4

吕功煊[1,*], 甄文龙[1,2]

(1. 中国科学院兰州化学物理研究所 羰基合成与选择氧化国家重点实验室,甘肃 兰州 730000;
2. 中国科学院大学,北京 100049)

摘要: 我们报道了在可见光照射下, 半导体硫化镉(CdS)悬浮体系在催化分解水制氢同时会伴随着少量氦-3 和氦-4 产生. 结果表明, 在温和条件下自水中的质子通过低能核反应(LENR)产生氦-3 和氦-4 的是可能的.

关键词: 光催化产氢; 生成氦-3 和氦-4; CdS 半导体悬浮体系; 可见光辐照